

Influence of investigator experience on reliability of adult acquired flatfoot deformity measurements using weightbearing computed tomography[☆]

Cesar de Cesar Netto^{a,b,c,*}, Delaram Shakoor^c, Eric J. Dein^d, Hanci Zhang^e,
Gaurav K. Thawait^c, Martinus Richter^f, James R. Ficke^d, Lew C. Schon^b, Weightbearing CT
International Study Group, Shadpour Demehri^c

^a Department of Foot and Ankle Surgery, Hospital for Special Surgery, New York, NY, USA

^b Department of Foot and Ankle Surgery, MedStar Union Memorial Hospital, Baltimore, MD, USA

^c Department of Radiology and Radiological Science, The Johns Hopkins University School of Medicine, Baltimore, MD, USA

^d Department of Orthopaedic Surgery, The Johns Hopkins University School of Medicine, Baltimore, MD, USA

^e Department of Orthopaedic Surgery, Duke University Hospital, Durham, NC, USA

^f Department for Foot and Ankle Surgery Nuremberg and Rummelsberg, Schwarzenbruck, Germany

ARTICLE INFO

Article history:

Received 10 November 2017

Received in revised form 23 February 2018

Accepted 5 March 2018

Keywords:

Adult acquired flatfoot deformity

Flatfoot

Measurement

Weightbearing

Weightbearing computed tomography

ABSTRACT

Background: Our purpose was to assess the reliability of measurements of adult-acquired flatfoot deformity (AAFD) taken by investigators of different levels of clinical experience using weightbearing computed tomography (WBCT).

Methods: Nineteen AAFD patients underwent WBCT. Three investigators with different levels of clinical experience made AAFD measurements in axial, coronal, and sagittal planes. Intra- and interobserver reliability were assessed. Mean values for each measurement were compared between investigators.

Results: After a training protocol, substantial to perfect intra- and interobserver reliability was observed for most measures, regardless of the investigator's experience level. Significant differences between investigators were observed in 2 of 21 measured parameters: medial cuneiform–first metatarsal angle ($P=0.003$) and navicular–medial cuneiform angle ($P=0.001$).

Conclusions: AAFD radiographic measurements can be performed reliably by investigators with different levels of clinical experience using WBCT.

Level of evidence: Level II, prospective comparative study.

© 2018 European Foot and Ankle Society. Published by Elsevier Ltd. All rights reserved.

1. Introduction

Adult acquired flatfoot deformity (AAFD) is a complex, 3-dimensional foot deformity involving failure of several static and dynamic biomechanical stabilizers [1]. Loss of the medial longitudinal arch, hindfoot valgus, and mid-/forefoot abduction are the main components of the deformity [2]. The posterior tibialis tendon (PTT) is the primary dynamic stabilizer of the medial longitudinal arch, and its dysfunction is commonly associated with AAFD [3]. Some authors consider AAFD a consequence of PTT dysfunction [4,5]. Body weight is distributed

abnormally on static stabilizers, including the spring ligament, deltoid complex, and sinus tarsi ligaments. Failure of these secondary structures leads to AAFD progression [6]. Other authors consider the bony deformity as primary, and PTT and other soft tissue failures as consequences [7–9].

Given the heterogeneous and complex pathophysiology of AAFD, staging systems have been developed to characterize its biomechanical derangement and optimize its treatment [4,5,10]. These staging systems use patients' symptoms, physical examinations, and imaging measurements obtained from conventional weightbearing radiographs [10]. Operative and nonoperative treatment guidelines

[☆] Investigation performed at The Johns Hopkins University, Baltimore, MD and Medstar Union Memorial Hospital, Baltimore, MD.

Martinus Richter, Alexej Barg, Francois Lintz, Cesar de Cesar Netto, Arne Burssens, Shadpour Demehri, Kris Buedts, Mark Easley, Scott J. Ellis, Alexandre L. Godoy-Santos, Bryan Den Hartog, Lew C. Schon

* Corresponding author at: Department of Foot and Ankle Surgery, Hospital for Special Surgery, 535 E 70th Street, New York, NY 10021, USA.

have been recommended for each stage, and treatment is tailored according to the severity and stage of AAFD [11]. In the initial and flexible stages, deformity is altered with load; therefore, weightbearing radiographs have been used widely to evaluate and determine AAFD stage [12]. Because of the 3-dimensional (3D) and complex relationships of small osseous structures of the foot, accurate assessment of subtle changes during weightbearing is challenging using 2-dimensional (2D) conventional radiographs [7,13,14] and usually requires a high level of clinical experience [10].

Weightbearing computed tomography (WBCT) is an emerging imaging modality that provides high-resolution 3D images and enables detailed assessment of tarsal bones during weightbearing [15,16]. WBCT may improve precision and accuracy of the characterization of AAFD. A recent study demonstrated the superior capability of WBCT to show the collapse in flexible AAFD compared with nonweightbearing WBCT and reported considerable reliability of measurements when performed by experts [13,16]. The objective of our study was to evaluate the intra- and interobserver reliability of AAFD measurements taken by investigators with different levels of clinical experience using WBCT images.

2. Material and methods

This study complied with the Health Insurance Portability and Accountability Act and the Declaration of Helsinki. All aspects of the study were approved by our institutional review board, and written informed consent was obtained from all participants.

2.1. Study design

In this prospective, dual-institution study, we recruited consecutive patients in our tertiary hospital clinics from September 2014 through June 2016. We included patients aged 18 years or older with a diagnosis of symptomatic, flexible AAFD. We excluded patients who were unable to stand independently for at least 40 s, those incapable of communicating effectively with clinical study personnel, and those with contraindications for standard CT scans.

2.2. Subjects

Nineteen patients (13 right feet, 6 left feet) were included in our study. The study group consisted of 11 men and 8 women, with a mean body mass index of 31 (range, 19–46) and a mean age of 52 (range, 20–88) years.

2.3. WBCT imaging technique

Imaging studies were conducted on a cone-beam WBCT extremity scanner (generation II, Carestream Health Inc., Rochester, NY). Participants were scanned in a physiological upright weightbearing position, standing with their feet at shoulder width and distributing their body weight equally between both lower extremities. We applied a protocol similar to that used in previous technical assessments [15–17]. The contrast-to-noise ratio per unit of dose within the boundaries of the CT was enhanced by 90 kVp and 72 mA (6 mA and 20 ms for each frame, 600 frame acquisition). The size-specific dose estimate for WBCT ankle imaging was calculated to be approximately 12 mGy.

A Farmer chamber in a stack of three 16-cm CT dose index phantoms was used to calculate the weighted CT dose index and was found to be approximately 15 mGy [11]. Images of 0.5 mm³ isotropic voxels were reconstructed using a bone algorithm.

2.4. Measurements

The raw 3D data were used to generate axial, sagittal, and coronal image slices that were transferred digitally into Vue

PACS software (Carestream Health, Inc., Rochester, NY) for computer-based measurements. Image annotations were eliminated, and a unique, random number was assigned to each study. The investigators consisted of a board-certified foot and ankle surgeon, an orthopaedic surgery resident, and a medical student. Each investigator completed a training protocol with 5 AAFD patients who were not included in the study. After the protocol, each observer performed the measurements twice, independently and blindly, using a dedicated software. The training protocol included a standardized assessment of the full data set of images; however, the final choice of which image to use to perform each measurement was made freely and independently by each observer. The second set of measurements was performed 30 days after the first assessment. Investigators were blinded to the patient's identification and other measurements, and the order of the patient images was randomized.

2.5. Axial plane measurements

The axial plane was defined as parallel to the horizontal plane, represented by the platform where the patient was standing, with the horizontal boundary of the images aligned to the axis of the first metatarsal bone. Two axial measurements were defined: the talonavicular coverage angle (Fig. 1A) [16,18] and the talus–first metatarsal angle (Fig. 1B) [19].

2.6. Coronal plane measurements

The coronal plane was defined as perpendicular to the horizontal plane, with the horizontal margins of the images perpendicularly aligned to the bimalleolar ankle axis. Nine coronal measurements were defined. The first 3 measurements involved the subtalar horizontal angle, which comprises the angle formed by the intersection of the horizontal line of the floor and the tangent line to the posterior facet of the talus. The angle was measured at 3 levels: 75%, anterior aspect (Fig. 1C); 50%, midpoint (Fig. 1D); and 25%, posterior aspect (Fig. 1E) of the posterior subtalar joint length. Positive values signified valgus alignment of the subtalar joint. The fourth measurement was the calcaneal-fibular distance, which was obtained by measuring the shortest distance between the superior or lateral surface of the calcaneus and the distal part of the fibula (Fig. 1F). The fifth measurement was the forefoot arch angle (Fig. 1G) [20]. A positive value showed a relative lower positioning of the fifth metatarsal to the medial cuneiform. The sixth measurement was the navicular to skin distance [20]. The seventh measurement was the navicular to floor distance (Fig. 1H). The eighth measurement was the medial cuneiform to skin distance. The ninth measurement was the medial cuneiform to floor distance (Fig. 1I).

2.7. Sagittal plane measurements

The sagittal plane was defined as perpendicular to the axial and coronal planes. The second metatarsal axis was used to determine the horizontal border of the images. Ten sagittal measurements were assessed. The first was calcaneal inclination angle (Fig. 1J) [21]. The second and third measurements were the navicular to floor and navicular to skin distances. The fourth and fifth measurements were the cuboid to floor (Fig. 1K) and to cuboid to skin distances [22]. The sixth and seventh measurements were the medial cuneiform to floor and medial cuneiform to skin distances [23–25]. The eighth measurement was the talus–first metatarsal angle (Fig. 1L). The ninth measurement was the medial cuneiform–first metatarsal angle, which was formed by the intersection of the axes of the first metatarsal and medial

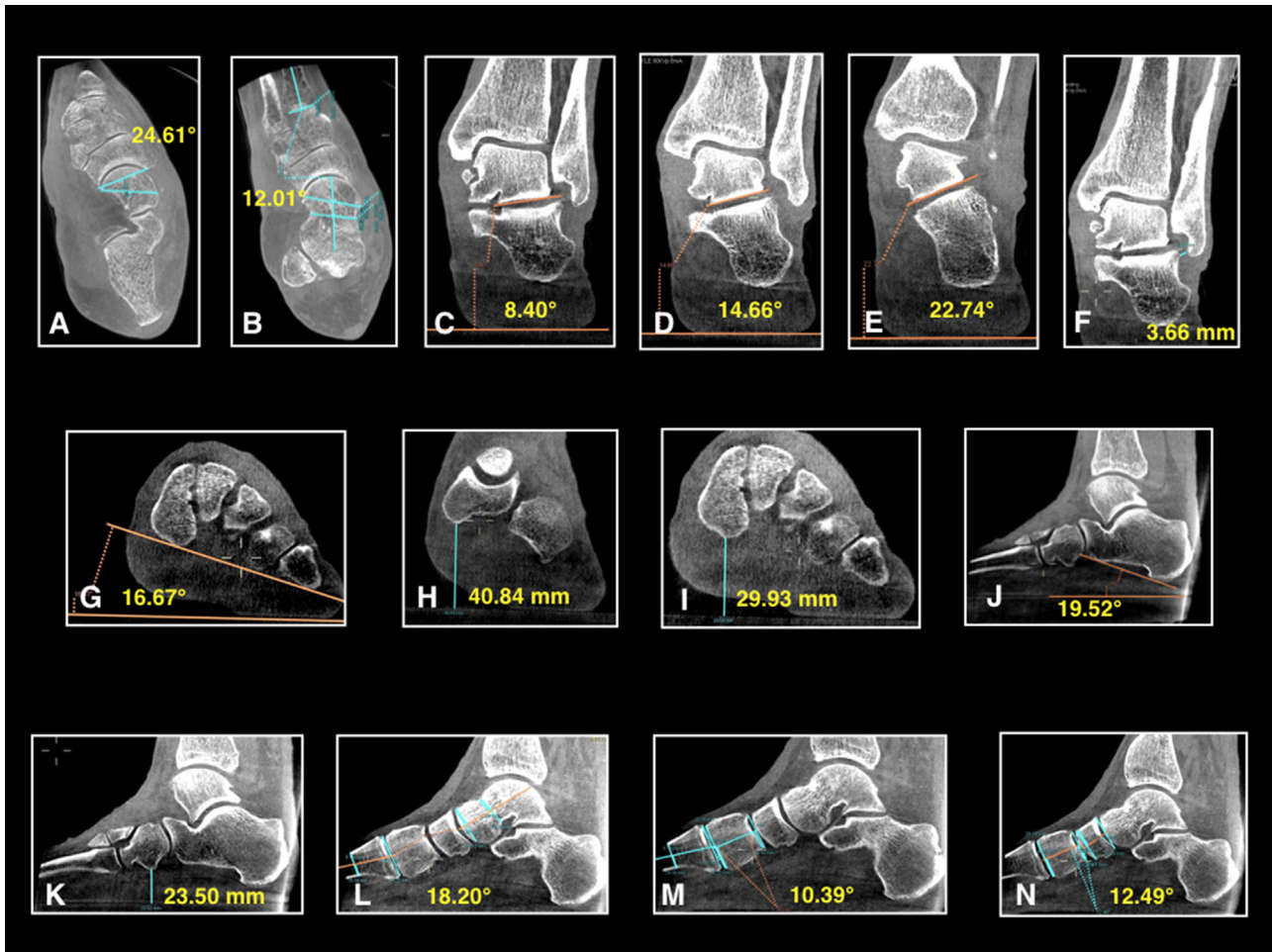


Fig. 1. Examples of measurements performed by 3 readers in 19 patients with adult acquired flatfoot deformity using weightbearing computed tomography. (A) Talonavicular coverage angle. (B) Talus–first metatarsal angle (axial plane). (C) Subtalar horizontal angle, 75% (posterior). (D) Subtalar horizontal angle, 50% (midpoint). (E) Subtalar horizontal angle, 25% (anterior). (F) Calcaneal–fibular distance. (G) Forefoot arch angle. (H) Navicular to floor distance. (I) Medial cuneiform to floor distance. (J) Calcaneal inclination angle. (K) Cuboid to floor distance. (L) Talus–first metatarsal angle (sagittal plane). (M) Medial cuneiform–first metatarsal angle. (N) Navicular–medial cuneiform angle.

cuneiform (Fig. 1M). The tenth measurement was the navicular–medial cuneiform angle, which was also created by the intersection of the axes of the navicular and medial cuneiform (Fig. 1N) [22].

The axis of short bones (i.e., navicular, medial cuneiform) was defined as a line connecting the midpoint of their proximal and distal articular surfaces. Because of a limitation in the field of view of the WBCT scan used in the study, the distal aspect of the first metatarsal could not be visualized, hindering the assessment of the true axis of the first metatarsal bone. An alternative standardized definition of the axis was used, represented by a line connecting the midpoint of the proximal articular surface and the midpoint of the width of the proximal third of the first metatarsal shaft.

2.8. Statistical analysis

We used the Shapiro–Wilk test to assess normality of the data distribution for each measurement. The intraobserver reliability of each measurement was determined using the Pearson or Spearman correlation test, depending on the normality of the data. Intraclass correlation coefficients (ICCs) were used to assess interobserver reliability. The extent to which bias and interaction factors can decrease the ICC was also considered. Correlations were categorized as excellent, >0.74 ; good, 0.60 – 0.74 ; fair, 0.40 – 0.59 ; and poor, <0.40 [22,26]. We also compared the means of each

measurement among the 3 readers using one-way ANOVA when the data distribution was normal. For non-normally distributed data, we used Kruskal–Wallis analysis. *P* values of less than 0.05 were considered significant.

3. Results

3.1. Intraobserver reliability

Intraobserver reliability for each of the 3 readers is listed in Table 1. All measurements showed significant intraobserver reliability ($P < 0.05$). Averaged values showed excellent intraobserver reliability for the board-certified foot and ankle surgeon ($r = 0.87$), orthopaedic resident ($r = 0.86$), and medical student ($r = 0.81$).

Medial cuneiform–first metatarsal angle (sagittal plane), navicular–medial cuneiform angle (sagittal plane), and talus–first metatarsal angle (coronal plane) showed the weakest reliability among all measurements.

3.2. Interobserver reliability

Interobserver reliability for each measurement is reported in Table 2. Good to excellent interobserver reliability was observed for most of the measurements performed. Talus–first metatarsal angle (in both axial and sagittal planes), talonavicular coverage angle (axial plane), navicular–medial cuneiform angle (sagittal

Table 1
Intraobserver reliability of measurements of adult acquired flatfoot deformity in 19 patients using weightbearing computed tomography.^a

Measurement by view	Board-certified foot and ankle surgeon		Orthopaedic surgery resident		Medical student	
	Pearson/Spearman <i>r</i>	<i>P</i>	Pearson/Spearman <i>r</i>	<i>P</i>	Pearson/Spearman <i>r</i>	<i>P</i>
Axial view						
Talonavicular coverage angle	0.72	0.003	0.70	0.005	0.55	0.023
Talus–first metatarsal angle	0.65	0.005	0.63	0.008	0.43	0.031
Coronal view						
Subtalar horizontal angle, 25%	0.91	<0.001	0.91	<0.001	0.87	<0.001
Subtalar horizontal angle, 50%	0.93	<0.001	0.88	<0.001	0.87	<0.001
Subtalar horizontal angle, 75%	0.88	<0.001	0.85	<0.001	0.85	<0.001
Forefoot arch angle	0.99	<0.001	0.97	<0.001	0.94	<0.001
Navicular to skin distance	0.99	<0.001	0.97	<0.001	0.96	<0.001
Navicular to floor distance	0.98	<0.001	0.99	<0.001	0.96	<0.001
Calcaneal-fibular distance	0.92	<0.001	0.93	<0.001	0.88	<0.001
Medial cuneiform to skin distance	0.99	<0.001	0.98	<0.001	0.96	<0.001
Medial cuneiform to floor distance	0.99	<0.001	0.98	<0.001	0.98	<0.001
Sagittal view						
Calcaneal inclination angle	0.95	<0.001	0.96	<0.001	0.85	<0.001
Navicular to floor distance	0.94	<0.001	0.96	<0.001	0.92	<0.001
Navicular to skin distance	0.92	<0.001	0.91	<0.001	0.88	<0.001
Cuboid to floor distance	0.96	<0.001	0.96	<0.001	0.90	<0.001
Cuboid to skin distance	0.95	<0.001	0.94	<0.001	0.90	<0.001
Medial cuneiform to floor distance	0.96	<0.001	0.95	<0.001	0.91	<0.001
Medial cuneiform to skin distance	0.98	<0.001	0.95	<0.001	0.90	<0.001
Talus–first metatarsal angle	0.73	0.004	0.74	0.003	0.70	0.004
Medial cuneiform–first metatarsal angle	0.41	0.032	0.33	0.040	0.33	0.034
Navicular–medial cuneiform angle	0.55	0.025	0.58	0.020	0.49	0.028
Averaged value	0.87		0.86		0.81	

^a Correlations were categorized as perfect agreement, 0.81–1.0; substantial, 0.61–0.80; moderate, 0.41–0.60; fair, 0.21–0.40; slight, 0.10–0.20; and poor, less than 0.10.

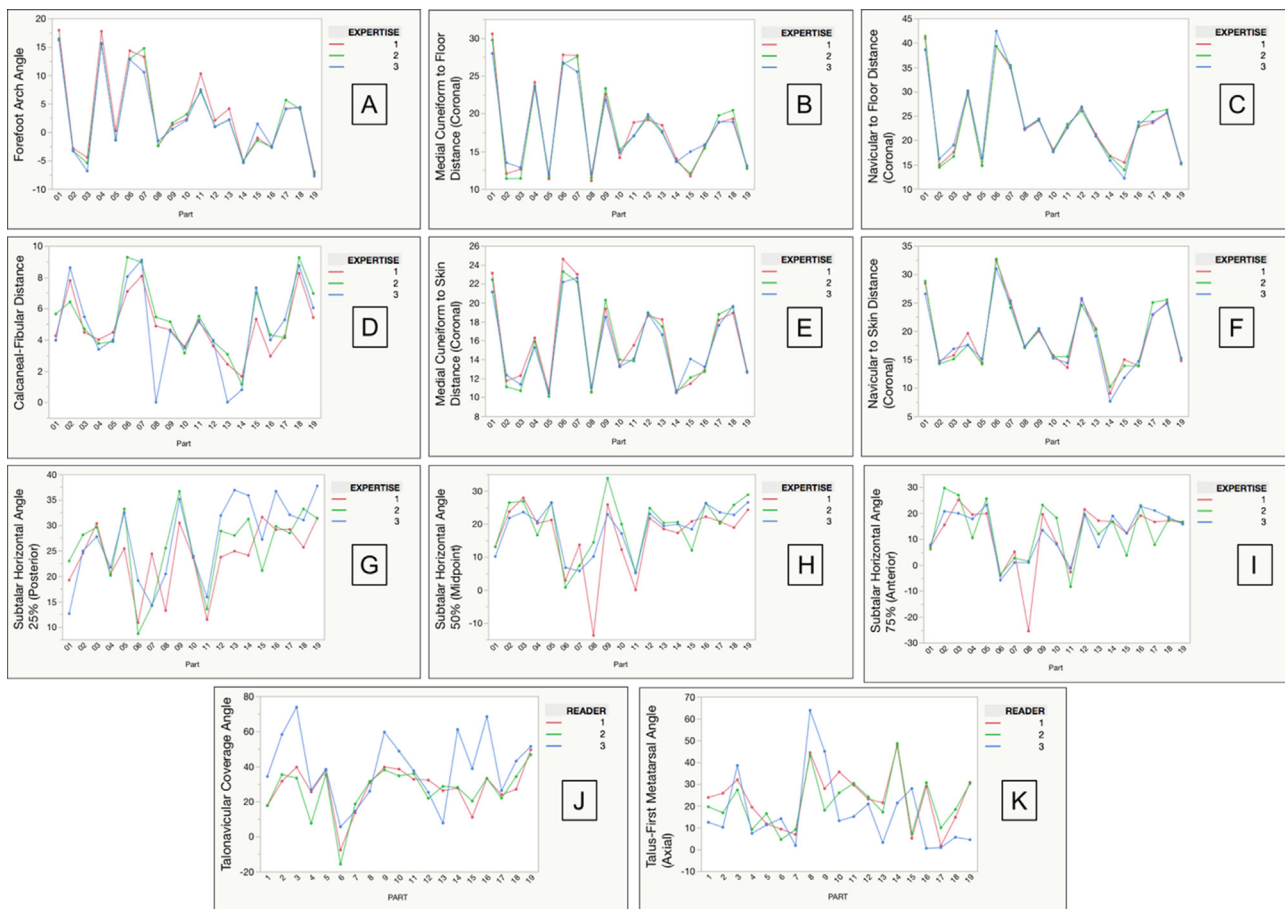


Fig. 2. Plots of interobserver agreement for measurements in the coronal and axial planes. Reader 1, board-certified foot and ankle surgeon; reader 2, orthopaedic surgery resident; and reader 3, medical student. (A) Forefoot arch angle (coronal plane). (B) Medial cuneiform to floor distance (coronal plane). (C) Navicular to floor distance (coronal plane). (D) Calcaneal-fibular distance (coronal plane). (E) Medial cuneiform to skin distance (coronal plane). (F) Navicular to skin distance (coronal plane). (G) Subtalar horizontal angle, 25% (posterior). (H) Subtalar horizontal angle, 50% (midpoint). (I) Subtalar horizontal angle, 75% (anterior). (J) Talonavicular coverage angle (axial plane). (K) Talus–first metatarsal angle (axial plane).

Table 2
Interobserver reliability of measurements of adult acquired flatfoot deformity in 19 patients using weightbearing computed tomography.^a

Measurement by view	Intraclass correlation	Classification
Axial view		
Talonavicular coverage angle	0.56	Fair
Talus–first metatarsal angle	0.53	Fair
Coronal view		
Subtalar horizontal angle, 25%	0.68	Good
Subtalar horizontal angle, 50%	0.74	Good
Subtalar horizontal angle, 75%	0.76	Excellent
Forefoot arch angle	0.98	Excellent
Navicular to skin distance	0.98	Excellent
Navicular to floor distance	0.99	Excellent
Calcaneal–fibular distance	0.76	Excellent
Medial cuneiform to skin distance	0.98	Excellent
Medial cuneiform to floor distance	0.98	Excellent
Sagittal view		
Calcaneal inclination angle	0.76	Excellent
Navicular to floor distance	0.96	Excellent
Navicular to skin distance	0.90	Excellent
Cuboid to floor distance	0.95	Excellent
Cuboid to skin distance	0.96	Excellent
Medial cuneiform to floor distance	0.94	Excellent
Medial cuneiform to skin distance	0.98	Excellent
Talus–first metatarsal angle	0.42	Fair
Medial cuneiform–first metatarsal angle	0.21	Poor
Navicular–medial cuneiform angle	0.37	Poor
Averaged value	0.78	Excellent

^a Correlations were categorized as excellent, >0.74; good, 0.60–0.74; fair, 0.40–0.59; and poor, <0.40.

plane) and medial cuneiform–first metatarsal angle (sagittal plane) had the weakest results, with only poor to fair reliability.

Plots of interobserver reliability are presented for measurements in the axial and coronal planes (Fig. 2) and in the sagittal plane (Fig. 3).

Table 3
Measurements in 19 patients with adult acquired flatfoot deformity performed by 3 investigators of varying expertise using weightbearing computed tomography.

Measurement by view	Board-certified foot and ankle surgeon		Orthopaedic resident		Medical student		P
	Mean	95% CI	Mean	95% CI	Mean	95% CI	
Axial view							
Talonavicular coverage angle, degrees	27.9	20.7, 35.1	26.8	19.4, 33.9	39.2	32.0, 46.4	0.032 ^d
Talus–first metatarsal angle, degrees	23.1	16.7, 29.6	21.4	15.0, 27.8	16.7	10.3, 23.1	0.111
Coronal view							
Subtalar horizontal angle 25%, degrees	23.8	20.5, 27.2	25.7	22.3, 29.1	27.2	23.8, 30.6	0.376
Subtalar horizontal angle 50%, degrees	16.4	12.3, 20.4	19.5	15.4, 23.5	18.4	14.4, 22.5	0.626
Subtalar horizontal angle 75%, degrees	11.9	6.95, 16.8	13.2	8.26, 18.1	12.7	7.82, 17.6	0.971
Forefoot arch angle, degrees	3.49	0.08, 6.91	2.91	–0.51, 6.32	2.61	–0.81, 6.02	0.935
Navicular to skin distance, mm	19.1	16.4, 21.9	19.1	16.4, 21.9	18.7	16.0, 21.5	0.993
Navicular to floor distance, mm	23.5	19.7, 27.2	23.5	19.8, 27.3	23.6	19.9, 27.4	0.988
Calcaneal–fibular distance, mm	4.86	3.80, 5.91	5.34	4.29, 6.41	4.83	3.77, 5.88	0.739
Medial cuneiform to skin distance, mm	15.9	13.9, 17.9	15.6	13.6, 17.7	15.5	13.5, 17.6	0.980
Medial cuneiform to floor distance, mm	18.0	15.4, 20.7	17.9	15.2, 20.5	17.9	15.3, 20.6	0.938
Sagittal view							
Calcaneal inclination angle, degrees	14.9	12.5, 17.3	14.0	11.6, 16.4	15.0	12.6, 17.3	0.818
Navicular to floor distance, mm	24.3	20.3, 28.2	23.3	19.3, 27.3	23.8	19.9, 27.8	0.954
Navicular to skin distance, mm	20.4	16.9, 23.9	19.0	15.5, 22.5	19.3	15.8, 22.8	0.952
Cuboid to floor distance, mm	17.2	15.1, 19.3	16.7	14.6, 18.7	17.3	15.2, 19.4	0.908
Cuboid to skin distance, mm	16.5	14.5, 18.5	15.9	13.9, 17.9	16.2	14.2, 18.3	0.967
Medial cuneiform to floor distance, mm	18.5	15.8, 21.3	17.9	15.1, 20.6	18.1	15.4, 20.9	0.984
Medial cuneiform to skin distance, mm	15.5	13.5, 17.5	15.2	13.2, 17.3	15.4	13.4, 17.5	0.945
Talus–first metatarsal angle, degrees	25.7	21.5, 29.9	29.0	24.8, 33.2	23.0	18.8, 27.2	0.127
Medial cuneiform–first metatarsal angle, degrees	3.39	0.19, 6.58	8.83	5.63, 12.0	1.61	–1.58, 4.81	0.003 ^{a,c}
Navicular–medial cuneiform angle, degrees	8.48	3.19, 13.8	18.6	13.3, 23.9	22.5	17.2, 27.8	0.001 ^{a,b}

CI: confidence interval.

^a Significant difference between surgeon and resident ($P < 0.05$).

^b Significant difference between surgeon and medical student ($P < 0.05$).

^c Significant difference between resident and medical student ($P < 0.05$).

^d Difference not confirmed in the post-hoc group comparison.

3.3. Measurement differences

Mean values, confidence intervals, and comparisons of each measurement among the 3 investigators are reported in Table 3. Of the 21 measurements, we observed significant differences among the investigators in only 2 measurements: the medial cuneiform–first metatarsal angle ($P = 0.003$) and navicular–medial cuneiform angle ($P = 0.001$). In the post-hoc group comparison, the medial cuneiform–first metatarsal angle measurements were different between the board-certified foot and ankle surgeon and the orthopaedic resident ($P = 0.003$) and between the orthopaedic resident and the medical student ($P = 0.005$). Navicular–medial cuneiform angle readings were different between the board-certified foot and ankle surgeon and the orthopaedic resident ($P = 0.0005$) and between the board-certified foot and ankle surgeon and the medical student ($P = 0.005$). We also found significant differences among the investigators for the talonavicular coverage angle measurements ($P = 0.032$). However, in the post-hoc group comparison that difference was not confirmed.

4. Discussion

To our knowledge, this is the first study to evaluate the reliability of traditional measurements of AAFD using high-resolution 3D WBCT by investigators of different levels of clinical experience. Our results show that, after training, most of the evaluated measurements can be performed reliably by a medical student, an orthopaedic resident, and a board-certified foot and ankle surgeon.

There has been a growing trend among foot and ankle surgeons to use WBCT in the assessment of patients with AAFD [12,20,22,27–31]. This imaging modality improves our understanding of this complex 3D deformity and overcomes challenges associated with the 2D biometrics of conventional radiographs [32]. Multiple radiographic measurements have been described to

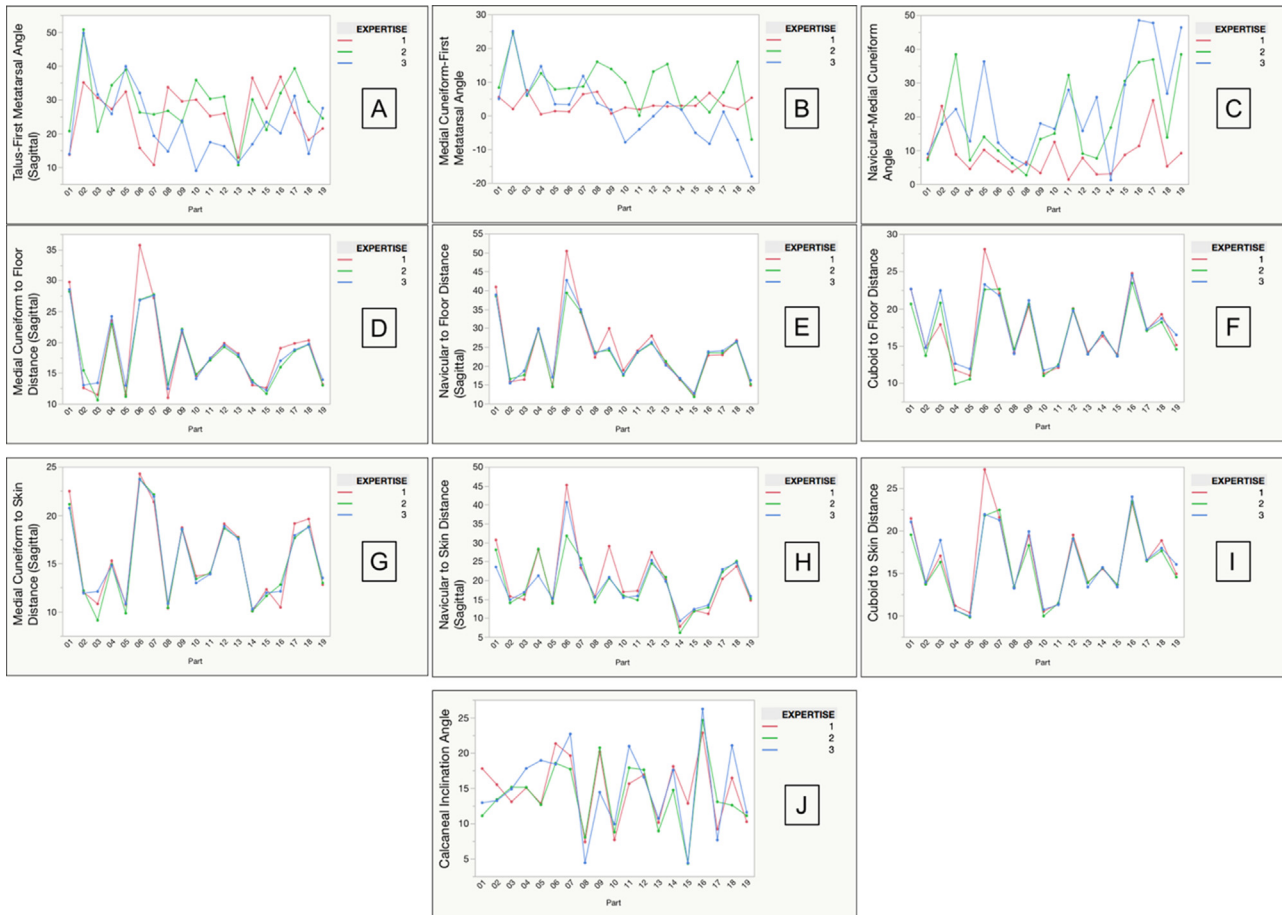


Fig. 3. Plots of interobserver agreement for measurements in the sagittal plane. Reader 1, board-certified foot and ankle surgeon; reader 2, orthopaedic surgery resident; and reader 3, medical student. (A) Talus–first metatarsal angle. (B) Medial cuneiform–first metatarsal angle. (C) Navicular–medial cuneiform angle. (D) Medial cuneiform to floor distance. (E) Navicular to floor distance. (F) Cuboid to floor distance. (G) Medial cuneiform to skin distance. (H) Navicular to skin distance. (I) Cuboid to skin distance. (J) Calcaneal inclination angle.

assist in the staging and operative treatment algorithm for AAFD, and their intra- and interobserver reliabilities have been reported [19]. Younger et al. [19] found the talus–first metatarsal angle in the lateral view (sagittal plane) to be the most consistently accurate measurement to differentiate AAFD patients from controls, with high intraobserver ($r=0.75$) and interobserver reliability ($r=0.83$). They also measured cuboid to floor and medial cuneiform to floor distances in the sagittal plane, with fair intraobserver reliability ($r=0.40$ and $r=0.51$, respectively) and excellent interobserver reliability ($r=0.96$ and 0.90 , respectively); calcaneal inclination angle, with good intraobserver reliability ($r=0.60$) and fair interobserver reliability ($r=0.54$); talus–first metatarsal angle in the anteroposterior view (axial plane), with excellent intra- ($r=0.76$) and interobserver reliability ($r=0.86$); and the talonavicular coverage angle, with poor intraobserver ($r=0.01$) and interobserver reliability ($r=0.30$) [19]. Similarly, Arunakul et al. [33] showed overall excellent intraobserver reliability and good to excellent interobserver reliability between an orthopaedic foot and ankle fellow and a biomechanical engineer. The authors measured the intraobserver and interobserver reliability of the talonavicular coverage angle (ICC=0.93 and 0.85, respectively), the talus–first metatarsal angle in the sagittal plane (ICC=0.96 and 0.69, respectively), and the calcaneal inclination angle (ICC=0.95 and 0.98, respectively) [33].

Sensiba et al. [10] were the first to evaluate the reliability of AAFD measurements with readers of different levels of clinical experience (medical student, junior and senior orthopaedic

residents) using conventional and digital weightbearing radiographs. They found substantial to perfect interobserver reliability for all evaluated measurements. Interobserver reliability was especially high for the medial cuneiform–fifth metatarsal distance in the sagittal plane (0.99), an alternative way of measuring medial column height, and the calcaneal inclination angle (0.95). The authors also found substantial to perfect intraobserver reliability, with overall better results favoring the more experienced residents, with r values ranging from 0.66–0.98 for the medical student, 0.77–0.98 for the junior resident, and 0.83–0.95 for the senior resident [10].

Ellis et al. [22] studied multiple AAFD measurements in patients with flexible deformity using weightbearing multiplanar CT images. They reported good to excellent interobserver reliability between 2 board-certified radiologists for the readings of the talus–first metatarsal angle in the axial and sagittal planes (0.84 and 0.82, respectively), forefoot arch angle (0.81), and medial cuneiform to floor distance in the sagittal view (0.93). The authors also found fair interobserver reliability for the talonavicular coverage angle (0.53), navicular to skin distance in the coronal plane (0.52), lateral gutter distance in the coronal plane (0.48) (a measurement that is similar to the calcaneal–fibular distance performed in our study), and the navicular–medial cuneiform angle in the sagittal plane (0.51). They concluded that most of the parameters typically assessed with conventional radiographs showed good to excellent ICC values for interobserver reliability when measured using multiplanar CT images. The authors also

proposed that the lower reliability in some of the measurements, especially those performed in the coronal plane, could be related to the fact that they are not commonly measured by radiologists. Probasco et al. [31] evaluated the subtalar joint alignment of patients with flexible AAFD and controls using weightbearing multiplanar CT. They found excellent intraobserver (ICC = 0.94) and interobserver reliability (ICC = 0.99) for the subtalar horizontal angle.

A recent study found that measurements analogous to traditional radiographic measurements of AAFD are obtainable using high-resolution WBCT imaging [16]. In that study, using only expert investigators (2 board-certified foot and ankle surgeons and 1 fellowship-trained radiologist), the authors showed increased severity of the deformity in weightbearing images compared with nonweightbearing images. They also found overall excellent intra- and interobserver reliability on weightbearing images ($r = 0.93$ and $ICC = 0.81$, respectively) [16]. However, the proper approach to obtaining the correct images and performing the measurements in a 3D imaging environment demands training and is extremely time-consuming, which may hinder its routine use in evaluating AAFD patients. We believe it is important to verify the quality and reproducibility of the measurements when performed by less experienced health care personnel.

When comparing the readings of 3 investigators of different levels of clinical expertise, we observed significant differences in the mean values for only 2 of 21 measurements performed (medial cuneiform–first metatarsal angle and navicular–medial cuneiform angle). Although it is impossible to determine which investigators made the correct measurements, the readings of the most experienced investigator were the ones that differed from those performed by the least experienced investigators. Similar to prior studies, we also found that measurement of linear distances is more reliable than measurement of angles, demonstrating higher intra- and interobserver reliability [16,19,22,33]. Measuring distances is simpler than measuring angles because angle measurements usually depend on a more complex process of finding particular bone axes. Measurements that involve the evaluation of the axis of the talus are even more difficult to perform reliably, demonstrating the challenges inherent in the complex 3D shape of this bone [16,17,19,22,33]. The positioning of the line representing the talar axis is technically demanding and seems to be sensitive to slight changes in the plane of the image used to perform a measurement [16].

Our study has several limitations. Although a standardized alternative assessment was used in the definition of the first metatarsal axis, the investigators were unable to see the whole length of the first metatarsal, especially its distal aspect, in sagittal and axial plane images. That represents a limitation in the field of view and imaging acquisition of the WBCT scanner used in the study. This could have influenced the adequate definition of the first metatarsal axis, hindering the measurement of the talus–first metatarsal and medial cuneiform–first metatarsal angles, likely affecting intra- and interobserver reliability. We also had a relatively small number of subjects involved in the study [19], and no power or sample size calculation was performed prospectively. However, our findings of significant intra- and interobserver correlations suggest adequate statistical power.

In conclusion, we found that AAFD measurements can be performed reliably by investigators with different levels of clinical experience using WBCT imaging, demonstrating overall good to excellent intra- and interobserver reliability.

Funding

This work was based on an industrial grant from Carestream, Inc. (Rochester, NY, US), which provides monetary incentive to subjects who undergo CBCT examinations.

Ethical approval

This study complied with the Health Insurance Portability and Accountability Act and the Declaration of Helsinki. All aspects of the study were approved by our institutional review board.

Informed consent

Written informed consent was obtained from all participants.

Conflict of interest

Dr. de Cesar Netto reports grants from Carestream Health, during the conduct of the study; and is a member and a part of the Board (Secretary) of the Weightbearing CT International Study Group.

Dr. Demehri reports grants from Carestream, Inc.

Dr. Thawait, Dr. Ficke, Dr. Shakoor and Dr. Zhang have nothing to disclose.

Dr. Richter reports:

- Paid consultancy for Curvebeam, Stryker, Geistlich and Intercus.
- Proprietor of R-Innovation.

Dr. Lew C. Schon reports:

- Item 1. Royalties from a company or supplier
- The following conflicts were disclosed
- Arthrex, Inc
- Darco
- DJ Orthopaedics
- Wright Medical Technology, Inc.
- Zimmer
- Item 2. Speakers bureau/paid presentations for a company or supplier
- The following conflicts were disclosed
- Biomet
- Tornier
- Wright Medical Technology, Inc.
- Zimmer
- Item 3A. Paid employee for a company or supplier
- No Conflict Reported
- Item 3B. Paid consultant for a company or supplier
- The following conflicts were disclosed
- Biomet
- Bonfix Ltd
- Guidepoint Global; Gerson Lehrman Group
- Spinesmith Celling Bioscience
- Tornier
- Wright Medical Technology, Inc.
- Zimmer
- Item 3C. Unpaid consultant for a company or supplier
- The following conflicts were disclosed
- Royer Biomedical, Inc; Carestream Health;
- Item 4. Stock or stock options in a company or supplier
- The following conflicts were disclosed
- Royer Biomedical Inc., Bioactive Surgical Inc., Healthpoint Capital
- Stem Cell Suture Company
- Wright Medical Technology, Inc.
- Item 5. Research support from a company or supplier as a PI The following conflicts were disclosed Biocomposites Biomet Bioventus Royer Biomedical, Inc
- spinesmith
- Synthes
- Zimmer

- Item 6. Other financial or material support from a company or supplier
- The following conflicts were disclosed
- Bioactive Surgical Inc
- Concepts in Medicine LLC
- OMEGA
- Smith & Nephew
- Item 7. Royalties, financial or material support from publishers
- The following conflicts were disclosed
- Elsevier (publishing textbook royalty)

References

- [1] Toullec E. Adult flatfoot. *Orthop Traumatol Surg Res OTSR* 2015;101(Suppl. 1):S11–7.
- [2] Peeters K, Schreuer J, Burg F, Behets C, Van Bouwel S, Dereymaeker G, et al. Altered talar and navicular bone morphology is associated with pes planus deformity: a CT-scan study. *J Orthop Res* 2013;31(2):282–7.
- [3] Basioni Y, El-Ganainy AR, El-Hawary A. Double calcaneal osteotomy and percutaneous tenoplasty for adequate arch restoration in adult flexible flat foot. *Int Orthop* 2011;35(1):47–51.
- [4] Johnson KA, Strom DE. Tibialis posterior tendon dysfunction. *Clin Orthop* 1989;239:196–206.
- [5] Myerson MS. Adult acquired flatfoot deformity. Treatment of dysfunction of the posterior tibial tendon. *J Bone Jt Surg Am Vol* 1996;78(5):780–92.
- [6] Lin YC, Mhuircheartaigh JN, Lamb J, Kung JW, Yablon CM, Wu JS. Imaging of adult flatfoot: correlation of radiographic measurements with MRI. *AJR Am J Roentgenol* 2015;204(2):354–9.
- [7] Richter M, Zech S. Lengthening osteotomy of the calcaneus and flexor digitorum longus tendon transfer in flexible flatfoot deformity improves talo-1st metatarsal-index: clinical outcome and pedographic parameter. *Foot Ankle Surg* 2013;19(1):56–61.
- [8] Deland JT. Adult-acquired flatfoot deformity. *J Am Acad Orthop Surg* 2008;16(7):399–406.
- [9] Cody EA, Williamson ER, Burket JC, Deland JT, Ellis SJ. Correlation of talar anatomy and subtalar joint alignment on weightbearing computed tomography with radiographic flatfoot parameters. *Foot Ankle Int* 2016;37(8):874–81.
- [10] Sensiba PR, Coffey MJ, Williams NE, Mariscalco M, Laughlin RT. Inter- and intraobserver reliability in the radiographic evaluation of adult flatfoot deformity. *Foot Ankle Int* 2010;31(2):141–5.
- [11] American Association of Physicists in Medicine. Comprehensive methodology for the evaluation of radiation dose in X-ray computed tomography. AAPM Report No. 111. Available at http://www.aapm.org/pubs/reports/RPT_111.pdf [Accessed 28 July 2017].
- [12] Kido M, Ikoma K, Imai K, Maki M, Takatori R, Tokunaga D, et al. Load response of the tarsal bones in patients with flatfoot deformity: in vivo 3D study. *Foot Ankle Int* 2011;32(11):1017–22.
- [13] Richter M, Seidl B, Zech S, Hahn S. PedCAT for 3D-imaging in standing position allows for more accurate bone position (angle) measurement than radiographs or CT. *Foot Ankle Surg* 2014;20(3):201–7.
- [14] Richter M, Zech S. Arthrorisis with calcaneostop screw in children corrects Talo-1st Metatarsal-Index (TMT-Index). *Foot Ankle Surg* 2013;19(2):91–5.
- [15] Carrino JA, Al Muhit A, Zbijewski W, Thawait GK, Stayman JW, Packard N, et al. Dedicated cone-beam CT system for extremity imaging. *Radiology* 2014;270(3):816–24.
- [16] de Cesar Netto C, Schon LC, Thawait GK, da Fonseca LF, Chinanuvathana A, Zbijewski WB, et al. Flexible adult acquired flatfoot deformity: comparison between weight-bearing and non-weight-bearing measurements using cone-beam computed tomography. *J Bone Jt Surg Am* 2017;99(18):e98.
- [17] Demehri S, Muhit A, Zbijewski W, Stayman JW, Yorkston J, Packard N, et al. Assessment of image quality in soft tissue and bone visualization tasks for a dedicated extremity cone-beam CT system. *Eur Radiol* 2015;25(6):1742–51.
- [18] Sangeorzan BJ, Mosca V, Hansen Jr. ST. Effect of calcaneal lengthening on relationships among the hindfoot, midfoot, and forefoot. *Foot Ankle Int* 1993;14(3):136–41.
- [19] Younger AS, Sawatzky B, Dryden P. Radiographic assessment of adult flatfoot. *Foot Ankle Int* 2005;26(10):820–5.
- [20] Ferri M, Scharfenberger AV, Goplen G, Daniels TR, Pearce D. Weightbearing CT scan of severe flexible pes planus deformities. *Foot Ankle Int* 2008;29(2):199–204.
- [21] Coughlin MJ, Kaz A. Correlation of Harris mats, physical exam, pictures, and radiographic measurements in adult flatfoot deformity. *Foot Ankle Int* 2009;30(7):604–12.
- [22] Ellis SJ, Deyer T, Williams BR, Yu JC, Lehto S, Maderazo A, et al. Assessment of lateral hindfoot pain in acquired flatfoot deformity using weightbearing multiplanar imaging. *Foot Ankle Int* 2010;31(5):361–71.
- [23] Iossi M, Johnson JE, McCormick JJ, Klein SE. Short-term radiographic analysis of operative correction of adult acquired flatfoot deformity. *Foot Ankle Int* 2013;34(6):781–91.
- [24] Arangio GA, Wasser T, Rogman A. Radiographic comparison of standing medial cuneiform arch height in adults with and without acquired flatfoot deformity. *Foot Ankle Int* 2006;27(8):636–8.
- [25] Chadha H, Pomeroy G, Manoli 2nd A. Radiologic signs of unilateral pes planus. *Foot Ankle Int* 1997;18(9):603–4.
- [26] Fleiss JL. Statistical methods for rates and proportions. New York, NY: Wiley, John and Sons, Inc.; 1981.
- [27] Apostle KL, Coleman NW, Sangeorzan BJ. Subtalar joint axis in patients with symptomatic peritalar subluxation compared to normal controls. *Foot Ankle Int* 2014;35(11):1153–8.
- [28] Colin F, Horn Lang T, Zwicky L, Hintermann B, Knupp M. Subtalar joint configuration on weightbearing CT scan. *Foot Ankle Int* 2014;35(10):1057–62.
- [29] Krahenbuhl N, Tschuck M, Bolliger L, Hintermann B, Knupp M. Orientation of the subtalar joint: measurement and reliability using weightbearing CT scans. *Foot Ankle Int* 2016;37(1):109–14.
- [30] Malicky ES, Crary JL, Houghton MJ, Agel J, Hansen Jr. ST, Sangeorzan BJ. Talocalcaneal and subfibular impingement in symptomatic flatfoot in adults. *J Bone Jt Surg Am Vol* 2002;84(11):2005–9.
- [31] Probasco W, Haleem AM, Yu J, Sangeorzan BJ, Deland JT, Ellis SJ. Assessment of coronal plane subtalar joint alignment in peritalar subluxation via weight-bearing multiplanar imaging. *Foot Ankle Int* 2015;36(3):302–9.
- [32] Hirschmann A, Pfirrmann CW, Klammer G, Espinosa N, Buck FM. Upright cone CT of the hindfoot: comparison of the non-weight-bearing with the upright weight-bearing position. *Eur Radiol* 2014;24(3):553–8.
- [33] Arunakul M, Amendola A, Gao Y, Goetz JE, Femino JE, Phisitkul P. Tripod index: a new radiographic parameter assessing foot alignment. *Foot Ankle Int* 2013;34(10):1411–20.